Inorg. Chem. **2008**, *47*, 11910−11919

Effects of Metal Coordination Geometry on Stabilization of Human Telomeric Quadruplex DNA by Square-Planar and Square-Pyramidal Metal Complexes

Anna Arola-Arnal,[†,§] Jordi Benet-Buchholz,[§] Stephen Neidle,[‡] and Ramón Vilar*[,†,§]

Department of Chemistry, Imperial College London, South Kensington, London SW7 2AZ, United Kingdom, CRUK Biomolecular Structure Group, The School of Pharmacy University of London, London WC1N 1AX, United Kingdom, and Institute of Chemical Research of Catalonia (ICIQ), Avgda. Països Catalans 16, 43007 Tarragona, Spain

Received September 10, 2008

A series of square-planar and square-based pyramidal metal complexes (metal = Ni^{2+}, Cu^{2+}, Zn^{2+}, and V^{4+}) with salphen and salen derivatives as ligands have been prepared. The X-ray crystal structures of three of these complexes are reported, giving insight into the geometric properties of the compounds. The interactions of these complexes with duplex and human telomeric quadruplex DNA have been studied by fluorescence resonance energy transfer (FRET), fluorescent intercalator displacement assay, and in one case circular dichroism. These studies have shown the square-planar metal complexes to be excellent quadruplex DNA stabilizers. In addition, FRET competition assays have shown the complexes to have a high degree of selectivity for the DNA quadruplex versus duplex DNA. These studies have allowed us to establish the most important features that metal complexes should have to interact selectively with quadruplex DNA. This will be of value in defining the best strategy to prepare metal complexes as potential anticancer drugs.

Introduction

Quadruplex DNA structures are formed from stacks of guanine tetrads that arise from hydrogen-bonding interactions of four in-plane guanine bases, between the Watson−Crick edge of one guanine and the Hoogsteen edge of its neighbor. These structures are further stabilized by electrostatic interactions between the guanine carbonyl groups and alkali metal cations (see Figure 1). It has been recently established that in the human genome there are ca. 300 000 guanine-rich sequences that can potentially form quadruplex DNA structures. Some of these sequences have been identified as potential targets for novel anticancer drugs. In particular, formation of quadruplexes in human telomeric DNA (which consists of the tandem repeat sequence TTAGGG) has been shown to be a novel approach for the inhibition of telomerase and the selective destabilization of telomere maintenance.[1−8]

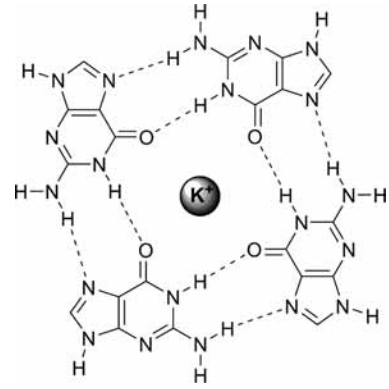

Figure 1. A guanine quartet highlighting the hydrogen bonding interactions between the Watson−Crick and Hoogsteen faces of the guanine bases, and the metal cation located at the center of the quartet.

This enzyme, which maintains telomere integrity, preventing the critical shortening of telomeric DNA, is overexpressed in 80−85% of cancer cells, in comparison to normal somatic

* Author to whom correspondence should be addressed. Telephone: +44-2075941967. E-mail: r.vilar@imperial.ac.uk.
† Imperial College London.
‡ The School of Pharmacy University of London.
§ ICIQ.

(1) Cairns, D.; Anderson, R. J.; Perry, P. J.; Jenkins, T. C. *Curr. Pharm. Des.* **2002**, *8*, 2491–2504.
(2) Cuesta, J.; Read, M. A.; Neidle, S. *Mini-Rev. Med. Chem.* **2003**, *3*, 11–21.

10.1021/ic8016547 CCC: $40.75
Published on Web 11/19/2008

Table 1. Crystal Data for Compounds **1**, **4**, and **15**

compound	**1**	**4**	**15**
formula	$C_{20}H_{18}N_2O_6Ni_1 \cdot 2H_2O$	$C_{43}H_{49.5}F_1N_4Ni_1O_4 \cdot 2\ C_6H_5CH_3$	$C_{20}H_{21}N_2O_{7.5}Zn_1 \cdot 3.5H_2O$
fw	441.07	764.08	474.76
cryst size (mm^3)	0.10 × 0.10 × 0.02	0.30 × 0.10 × 0.02	0.08 × 0.06 × 0.06
cryst color	red	red	yellow
cryst syst	monoclinic	orthorhombic	trigonal
space group	*C*2/*c*	*Iba*2	$P3_1$
a (Å)	10.8940(5)	26.765(4)	19.0583(10)
b (Å)	17.6520(8)	31.067(4)	19.0583(10)
c (Å)	9.0521(4)	9.5837(13)	4.9557(6)
α (deg)	90	90	90.00
β (deg)	101.286(1)°	90	90.00
γ (deg)	90	90	120.00
V ($Å^3$)	1707.07(13)	7969.2(18)	1558.8(2)
Z	4	8	3
ρ (g/cm^3)	1.716	1.274	1.517
μ (mm^{-1})	1.182	0.538	1.229
θ_{max} (deg)	39.52	23.36	39.16
reflns measured	16735	17985	29758
unique reflns	4960 [R_{int} = 0.0361]	5061 [R_{int} = 0.0563]	8825 [R_{int} = 0.0729]
abs correct.	SADABS (Bruker)	SADABS (Bruker)	SADABS (Bruker)
trans. min/max	0.8005/1.0000	0.5867/1.0000	0.5867/1.0000
parameters	168	476	291
R1/wR2 [$I > 2\sigma(I)$]	0.0283/0.0802	0.0821/0.2387	0.0470/0.1177
R1/wR2 [all data]	0.0335/0.0824	0.1128/0.2681	0.0579/0.1233
goodness-of-fit (F^2)	1.084	1.055	1.025
peak/hole ($e/Å^3$)	0.591/−0.551	0.794/−0.608	1.171/−0.503

cells, and plays an important part in cancer cell immortalization. Since the substrate of telomerase is the 3′-single-stranded overhang of telomeric DNA, molecules that stabilize quadruplex structures in the telomere can lead to inhibition of this enzyme.

A rational approach to designing molecules with optimal properties for quadruplex DNA stabilization has been established from crystallographic studies,[9−12] NMR spectroscopy,[13−19] and computer modeling.[20−27] For example, planar *π*-delocalized molecules able to stack on the face of the G-quartet have been demonstrated to be effective quadruplex binders. A partial positive charge on the molecule positioned at the center of the G-quartet has been shown to increase electrostatic stabilization by substituting the cationic charge of the potassium or sodium that would normally occupy the central quadruplex ion channel. In addition, the interaction of planar molecules with quadruplex DNA can be enhanced by substituents bearing a positive charge; it has been shown that such substituents can interact favorably with the grooves and loops of DNA and with the negatively charged backbone phosphates.

(3) De Cian, A.; Lacroix, L.; Douarre, C.; Temime-Smaali, N.; Trentesaux, C.; Riou, J.-F.; Mergny, J.-L. *Biochimie* **2008**, *90*, 131–155.
(4) Kelland, L. R. *Eur. J. Cancer* **2005**, *41*, 971–979.
(5) Kyo, S.; Inoue, M. *Curr. Med. Chem.* **2002**, *2*, 613–626.
(6) Mergny, J.-L.; Helene, C. *Nat. Med. (New York, N.Y., U.S.)* **1998**, *4*, 1366–1367.
(7) Rezler, E. M.; Bearss, D. J.; Hurley, L. H. *Curr. Opin. Pharmacol.* **2002**, *2*, 415–423.
(8) Rezler, E. M.; Bearss, D. J.; Hurley, L. H. *Annu. Rev. Pharmacol. Toxicol.* **2003**, *43*, 359–379.
(9) Clark, G. R.; Pytel, P. D.; Squire, C. J.; Neidle, S. *J. Am. Chem. Soc.* **2003**, *125*, 4066–4067.
(10) Campbell, N. H.; Parkinson, G. N.; Reszka, A. P.; Neidle, S. *J. Am. Chem. Soc.* **2008**, *130*, 6722–6724.
(11) Haider, S. M.; Parkinson, G. N.; Neidle, S. *J. Mol. Biol.* **2003**, *326*, 117–125.
(12) Parkinson, G. N.; Ghosh, R.; Neidle, S. *Biochemistry* **2007**, *46*, 2390–2397.
(13) Dai, J.; Punchihewa, C.; Ambrus, A.; Chen, D.; Jones, R. A.; Yang, D. *Nucleic Acids Res.* **2007**, *35*, 2440–2450.
(14) Escaja, N.; Gomez-Pinto, I.; Pedroso, E.; Gonzalez, C. *J. Am. Chem. Soc.* **2007**, *129*, 2004–2014.
(15) Hounsou, C.; Guittat, L.; Monchaud, D.; Jourdan, M.; Saettel, N.; Mergny, J.-L.; Teulade-Fichou, M.-P. *ChemMedChem* **2007**, *2*, 655–666.
(16) Ida, R.; Wu, G. *J. Am. Chem. Soc.* **2008**, *130*, 3590–3602.
(17) Patel, D. J.; Phan, A. T.; Kuryavyi, V. *Nucleic Acids Res.* **2007**, *35*, 7429–7455.
(18) Phan, A. T.; Modi, Y. S.; Patel, D. J. *J. Mol. Biol.* **2004**, *338*, 93–102.
(19) Webba da Silva, M. *Methods* **2007**, *43*, 264–277.
(20) Clay, E. H.; Gould, I. R. *J. Mol. Graphics Modell.* **2005**, *24*, 138–146.
(21) Hazel, P.; Huppert, J.; Balasubramanian, S.; Neidle, S. *J. Am. Chem. Soc.* **2004**, *126*, 16405–16415.
(22) Hazel, P.; Parkinson, G. N.; Neidle, S. *Nucleic Acids Res.* **2006**, *34*, 2117–2127.
(23) Ishikawa, Y.; Tomisugi, Y.; Uno, T. *Nucleic Acids Symp. Ser.* **2006**, 331–332.
(24) Sponer, J.; Spackova, N. *Methods* **2007**, *43*, 278–290.
(25) Virno, A.; Zaccaria, F.; Virgilio, A.; Esposito, V.; Galeone, A.; Mayol, L.; Randazzo, A. *Nucleosides, Nucleotides Nucleic Acids* **2007**, *26*, 1139–1143.
(26) Yang, D.-Y.; Chang, T.-C.; Sheu, S.-Y. *J. Phys. Chem. A* **2007**, *111*, 9224–9232.
(27) Ying, L.; Green, J. J.; Li, H.; Klenerman, D.; Balasubramanian, S. *Proc. Natl. Acad. Sci. U. S. A.* **2003**, *100*, 14629–14634.
(28) Brassart, B.; Gomez, D.; De Cian, A.; Paterski, R.; Montagnac, A.; Qui, K.-H.; Temime-Smaali, N.; Trentesaux, C.; Mergny, J.-L.; Gueritte, F.; Riou, J.-F. *Mol. Pharmacol.* **2007**, *72*, 631–640.
(29) Casals, J.; Debethune, L.; Alvarez, K.; Risitano, A.; Fox, K. R.; Grandas, A.; Pedroso, E. *Bioconjugate Chem.* **2006**, *17*, 1351–1359.
(30) Chakraborty, T. K.; Arora, A.; Roy, S.; Kumar, N.; Maiti, S. *J. Med. Chem.* **2007**, *50*, 5539–5542.
(31) Cheng, M.-K.; Modi, C.; Cookson, J. C.; Hutchinson, I.; Heald, R. A.; McCarroll, A. J.; Missailidis, S.; Tanious, F.; Wilson, W. D.; Mergny, J.-L.; Laughton, C. A.; Stevens, M. F. G. *J. Med. Chem.* **2008**, *51*, 963–975.
(32) Cuenca, F.; Greciano, O.; Gunaratnam, M.; Haider, S.; Munnur, D.; Nanjunda, R.; Wilson, W. D.; Neidle, S. *Bioorg. Med. Chem. Lett.* **2008**, *18*, 1668–1673.
(33) De Cian, A.; DeLemos, E.; Mergny, J.-L.; Teulade-Fichou, M.-P.; Monchaud, D. *J. Am. Chem. Soc.* **2007**, *129*, 1856–1857.
(34) De Cian, A.; Mergny, J.-L. *Nucleic Acids Res.* **2007**, *35*, 2483–2493.

Scheme 1. Synthetic Scheme for the Preparation of Nickel(II)−Salphen Complexes

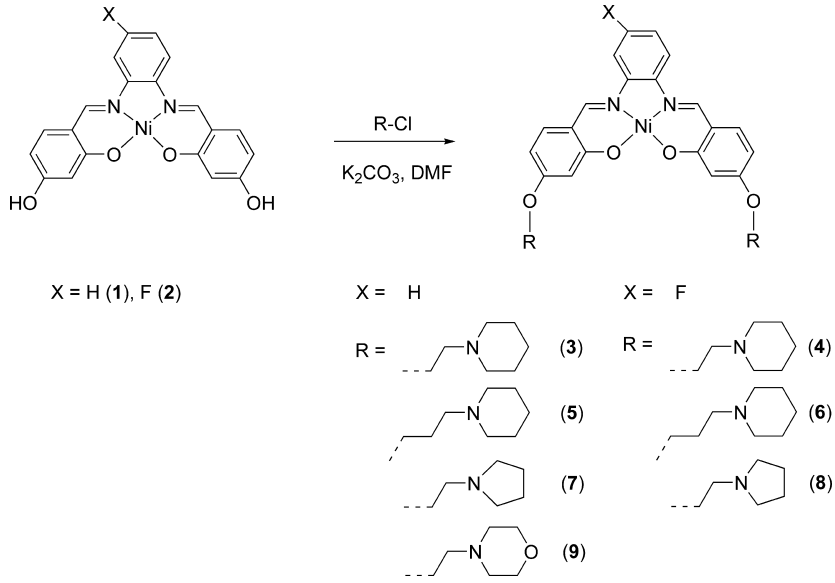

Most of the quadruplex DNA binders reported to date are based on organic heteroaromatic systems.[28−45] More recently, we[46,47] and others[35,48−51] have shown that metal complexes can be excellent stabilizers of quadruplex DNA. A metal coordinated to heteroaromatic multidentate ligands with a square-planar geometry can have several advantages over more "classical" quadruplex DNA binders. The metal can play a major structural role in organizing the ligand(s) into an optimal conformation for quadruplex DNA interaction. In addition, the electropositive metal can in principle be positioned at the center of the guanine quartet, increasing electrostatic stabilization by substituting the cationic charge of the potassium or sodium that would normally occupy this site. Another advantage is the electron-withdrawing properties of the metal, which reduce the electron density on the coordinated ligand, yielding a system that can display stronger $\pi-\pi$ interactions.

We recently reported in a preliminary communication that the planar nickel(II)−salphen complexes **3** and **4** (see Scheme 1) are excellent quadruplex DNA binders and telomerase inhibitors.[46] Herein, we present a detailed study of the interactions of a series of metal complexes analogous to **3** and **4** with DNA. In particular, we have examined the effects of differing metals and their corresponding coordination geometry on both quadruplex and duplex DNA affinity.

Experimental Section

Materials, Methods, and Instrumentation. Infrared spectra were recorded on a Thermo Nicolet 5700 or Perkin-Elmer FTIR 1720 spectrometer as KBr discs between 4000 and 400 cm^{-1}. All dry solvents were recovered using a solvent purification system. ^1H NMR and ^{13}C NMR spectra were recorded on an AM-400, Bruker Avance 400, AM-500, or Bruker Avance 500 spectrometer at room temperature. Compounds **1**−**4** were prepared following the procedure reported in our previous communication.[46] Compound **10** was prepared following a procedure previously reported.[52]

Synthesis. A detailed synthetic procedure and full characterization of all the compounds herein reported can be found in the Supporting Information.

Stock Solution Preparation. The following stock solutions were prepared and used in the fluorescence resonance energy transfer (FRET), circular dichroism (CD), and G4-fluorescent intercalator displacement (FID) studies. Complexes **3** and **4** were dissolved in a mixture of DMSO (75% by volume), H_2O (20%), and 1 mM HCl (5%) to give an 8 mM stock solution. Complexes **7**, **8**, **9**, **12**,

(35) Dixon, I. M.; Lopez, F.; Esteve, J.-P.; Tejera, A. M.; Blasco, M. A.; Pratviel, G.; Meunier, B. *ChemBioChem* **2005**, *6*, 123–132.
(36) Dixon, I. M.; Lopez, F.; Tejera, A. M.; Esteve, J.-P.; Blasco, M. A.; Pratviel, G.; Meunier, B. *J. Am. Chem. Soc.* **2007**, *129*, 1502–1503.
(37) Gomez, D.; Paterski, R.; Lemarteleur, T.; Shin-ya, K.; Mergny, J.-L.; Riou, J.-F. *J. Biol. Chem.* **2004**, *279*, 41487–41494.
(38) Goncalves, D. P. N.; Rodriguez, R.; Balasubramanian, S.; Sanders, J. K. M. *Chem. Commun.* **2006**, 4685–4687.
(39) Harrison, R. J.; Cuesta, J.; Chessari, G.; Read, M. A.; Basra, S. K.; Reszka, A. P.; Morrell, J.; Gowan, S. M.; Incles, C. M.; Tanious, F. A.; Wilson, W. D.; Kelland, L. R.; Neidle, S. *J. Med. Chem.* **2003**, *46*, 4463–4476.
(40) Moorhouse, A. D.; Haider, S.; Gunaratnam, M.; Munnur, D.; Neidle, S.; Moses, J. E. *Mol. Biosystems* **2008**, *4*, 629–642.
(41) Moorhouse, A. D.; Santos, A. M.; Gunaratnam, M.; Moore, M.; Neidle, S.; Moses, J. E. *J. Am. Chem. Soc.* **2006**, *128*, 15972–15973.
(42) Rezler, E. M.; Seenisamy, J.; Bashyam, S.; Kim, M.-Y.; White, E.; Wilson, W. D.; Hurley, L. H. *J. Am. Chem. Soc.* **2005**, *127*, 9439–9447.
(43) Shirude, P. S.; Gillies, E. R.; Ladame, S.; Godde, F.; Shin-ya, K.; Huc, I.; Balasubramanian, S. *J. Am. Chem. Soc.* **2007**, *129*, 11890–11891.
(44) Teulade-Fichou, M.-P.; Carrasco, C.; Guittat, L.; Bailly, C.; Alberti, P.; Mergny, J.-L.; David, A.; Lehn, J.-M.; Wilson, W. D. *J. Am. Chem. Soc.* **2003**, *125*, 4732–4740.
(45) Waller, Z. A. E.; Shirude, P. S.; Rodriguez, R.; Balasubramanian, S. *Chem. Commun.* **2008**, 1467–1469.
(46) Reed, J. E.; Arnal, A. A.; Neidle, S.; Vilar, R. *J. Am. Chem. Soc.* **2006**, *128*, 5992–5993.
(47) Reed, J. E.; Neidle, S.; Vilar, R. *Chem. Commun.* **2007**, 4366–4368.
(48) Bertrand, H.; Bombard, S.; Monchaud, D.; Teulade-Fichou, M.-P. *J. Biol. Inorg. Chem.* **2007**, *12*, 1003–1014.
(49) Bertrand, H.; Monchaud, D.; De Cian, A.; Guillot, R.; Mergny, J.-L.; Teulade-Fichou, M.-P. *Org. Biomol. Chem.* **2007**, *5*, 2555–2559.
(50) Evans, S. E.; Mendez, M. A.; Turner, K. B.; Keating, L. R.; Grimes, R. T.; Melchoir, S.; Szalai, V. A. *J. Biol. Inorg. Chem.* **2007**, *12*, 1235–1249.
(51) Kieltyka, R.; Fakhoury, J.; Moitessier, N.; Sleiman, H. F. *Chem.—Eur. J.* **2008**, *14*, 1145–1154.
(52) Deligoenuel, N.; Tuemer, M.; Serin, S. *Transition Met. Chem. (Dordrecht, Neth.)* **2006**, *31*, 920–929.

17, **14**, and **19** were dissolved in DMSO to give a 10 mM stock solution. Complexes **5** and **6** were dissolved in methanol to give a 5 mM stock solution. All solutions were stored at −20 °C and defrosted and diluted immediately before use.

Oligonucleotides. All oligonucleotides and their fluorescent conjugates were purchased from Eurogentec (U.K.). For the telomeric G4 DNA, the 22-mer double-labeled oligonucleotide F21T, 5′-FAM-dGGG(TTAGGG)$_3$-TAMRA-3′ (donor fluorophore FAM, 6-carboxyfluorescein; acceptor fluorophore TAMRA, 6-carboxy-tetramethylrhodamine) was used for FRET and FRET competition assays. The 22-mer 5′-AGGGTTAGGGTTAGGGTTAGGG-3′ was used in G4-FID studies, and the 26-mer 5′-GGATTGGGATTGGGATTGGGATTGGG-3′ was used in CD studies. For the duplex DNA, the double-labeled t-loop, 5′-FAM-TAT AGC TAT A TTT TTT T ATA GCT ATA-TAMRA-3′, was used in the FRET assay; the DNA sodium salt from calf thymus, CT DNA (Sigma-Aldrich), was used in the FRET competition assay.

FRET Measurements. Labeled oligos (see above) were dissolved as a stock 20 μM solution in MilliQ water and then annealed at a 400 nM concentration in a 60 mM potassium cacodylate buffer (pH 7.4) at 85 °C for 10 min and allowed to cool slowly to room temperature overnight. Compounds were dissolved from stock solutions (see above) to final concentrations in a 60 mM potassium cacodylate buffer (pH 7.4). Each well of a 96-well plate (MJ Research, Waltham, MA) contained 200 nM oligo and compound to test. Measurements were performed on a DNA Opticon PCR instrument (MJ Research) with excitation at 450−495 nm and detection at 515−545 nm. Readings were taken from 30 to 100 °C at intervals of 0.5 °C, maintaining a constant temperature for 30 s before each reading.

FRET Competition Studies. Two different buffers were used for this assay: (a) a mixture of 10 mM potassium cacodylate and 50 mM lithium cacodylate as the buffer (pH 7.4) and (b) a 60 mM potassium cacodylate buffer (pH 7.4). Buffer a was used for all dilutions when complexes **5**, **7**, **8**, and **9** were studied. Buffer b was used for all dilutions when complexes **12**, **14**, **17**, and **19** were investigated. F21T oligo (see above) was dissolved as a stock 20 μM solution in MilliQ water, then annealed as a 400 nM concentration in the buffer at 85 °C for 10 min, and allowed to cool slowly to room temperature overnight. A 10% w/v solution of CT DNA (see above) in the buffer was stirred gently over 3 days and then centrifuged for 3 min (1200 rpm) to remove nonsoluble oligo. The concentration and purity of the supernatant was determined by absorbance reading on a CARY 300 BIO UV−visible spectrophotometer and then diluted to correct concentrations. Compounds were dissolved from stock solutions (see above) to final concentrations in the buffer. Each well of a 96-well plate (MJ Research, Waltham, MA) was prepared with a final 200 nM oligo concentration, 1 μM compound concentration, and the CT DNA concentration to test. Measurements were performed under the same conditions as the FRET assay (see above).

Fluorescent Intercalator Displacement (G4-FID) Measurements. Oligos (see above) were dissolved as a stock 20 μM solution in MilliQ water, annealed to 0.5 μM concentration in a 60 mM potassium cacodylate buffer (pH 7.4) at 85 °C for 10 min, and allowed to cool slowly to room temperature overnight. Thiazole Orange (TO; Sigma-Aldrich) was freshly prepared as a 10 mM stock solution in DMSO. Compounds and TO were dissolved from stock solutions (see above) to the final concentration in a 60 mM potassium cacodylate buffer (pH 7.4). Measurements were performed at a final 0.25 μM concentration of oligo, 0.5 μM concentration of TO, and a compound concentration to test. Samples were left to stand for 3 min before measurements. Data were acquired at room temperature over a range of 515−748 nm with excitation at 501 nm.

Circular Dichroism (CD) Spectroscopy. Two different buffers were employed in this study: (a) 50 mM Tris-HCl and 150 mM KCl buffer (pH 7.4) and (b) 50 mM Tris-HCl buffer (pH 7.4) with no added KCl. The corresponding oligo (see above) was dissolved as a stock 100 μM solution in MilliQ. The oligo and compound **7** were dissolved from stock solutions (see above) to the final concentration in either of the two buffers. Measurements were performed using a 1:2 oligo/compound ratio. The CD spectra of the solutions were acquired on an Applied Photophysics Ltd. (Leatherhead, U.K.) Chirascan spectrometer. The CD spectra were measured in the wavelength region of 700−180 nm in a strain-free 10 mm × 2 mm rectangular cell path length. The instrument was flushed continuously with pure evaporated nitrogen throughout the experiment. Spectra were recorded with the following parameters: bandwidth, 1 nm; spectral range, 180−360 nm; step-size, 0.5 nm; time-pep-point, 1.5 s; smooth factor, 7. All spectra were buffer-baseline-corrected and measured at 20 °C. The UV and CD spectra were smoothed with window factors of 7 and 17 using the Savitsky-Golay method

X-Ray Crystallography. Complexes **1** and **4** crystallized as red single crystals from acetonitrile at room temperature. Complex **15** crystallized as yellow needles from methanol at room temperature. The measured crystals were prepared under inert conditions immersed in perfluoropolyether as the protecting oil for manipulation. Measurements were made on a Bruker-Nonius diffractometer equipped with an APPEX 2 4K CCD area detector, a FR591 rotating anode with Mo Kα radiation, Montel mirrors as the monochromator, and a Kryoflex low-temperature device ($T = -173$ °C). Full-sphere data collection was used with ω and φ scans. The programs used were as follows: data collection, Apex2 V.1.0−22 (Bruker-Nonius 2004); data reduction, Saint+ version 6.22 (Bruker-Nonius 2001); and absorption correction, SADABS V.2.10 (2003). SHELXTL version 6.10 (Sheldrick, 2000) was used for the structure solution and refinement.

Crystal structure solution was achieved using direct methods as implemented in SHELXTL version 6.10 (Sheldrick, Universität Göttingen, Germany, 2000) and visualized using the XP program. Missing atoms were subsequently located from difference Fourier synthesis and added to the atom list. Least-squares refinement on F2 using all measured intensities was carried out using the program SHELXTL version 6.10 (Sheldrick, Universität Göttingen, Germany, 2000). All non-hydrogen atoms were refined, including anisotropic displacement parameters. Hydrogen atoms were calculated in their idealized positions and were refined with a riding model. Hydrogen atoms at water molecules were located from the difference Fourier synthesis, added to the atom list, and refined in fixed positions. The hydrogen isotropic displacement parameters were constrained applying an equivalent isotropic displacement parameter of the carbon, nitrogen, or oxygen atom where the hydrogen atom rides.

Compound **4**, which was refined in the orthorhombic space group *Iba*2, crystallizes disordered with a fluorine atom located in the corresponding positions attached to C10 and C11 and with a ratio of 55:45. The piperidine groups show large thermal ellipsoids due to conformational disorder. The compound crystallizes as a toluene solvate with one and one-quarter molecules in the unit cell. The toluene molecules are partially disordered with large thermal displacement parameters. One of the toluene molecules is located on a 2-fold rotation axis and corresponds to a half molecule in the unit cell with an occupancy of 0.5. This corresponds to one-quarter

Scheme 2. Synthetic Scheme for the Preparation of Nickel(II)−Salen Complexes

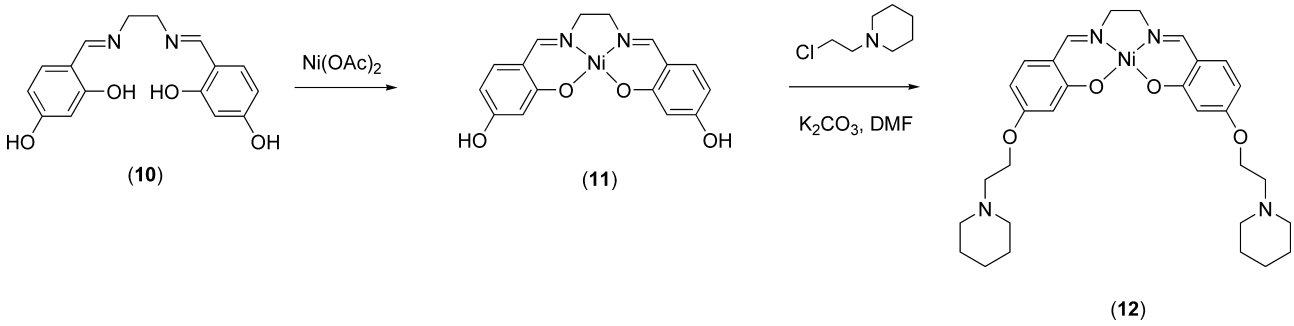

of a molecule for each metal complex. The occupancy of the carbon atoms of this last toluene molecule refined with the best *R* values when it was fixed at 0.5. The methyl group of the toluene molecule located on the rotation axis is disordered in two positions over the symmetry operation. All of the atoms of this toluene molecule were refined isotropically.

For compound **15**, which was refined in the trigonal space group $P3_1$, disordered positions for water molecules were located on the difference Fourier maps inside of a tube centered on the 3_1 axis (see Figure S24 in the Supporting Information). Additionally, one water molecule was detected that was coordinated to the metal atom. The occupancy ratios of the noncoordinated oxygen atoms were first free-refined with fixed isotropic *U* values. Later, the atoms were refined anisotropically with fixed occupancy values at 0.5 and 1.0, according to the proximity of these values to the approximated refined occupancies. This fixed occupancy ratios were refined giving the best R1 values. One of these water molecules has an occupancy of 1, while the other three are positionally disordered, having occupancy of 0.5. In total, the unit cell contains 3.5 molecules of water.

Results and Discussion

Design and Synthesis of Metal Complexes. Qualitative computer modeling was initially employed for the design of the metal complexes under study.[46] Qualitative in silico docking of a series of metal−salphen planar complexes with the human parallel intramolecular quadruplex telomeric DNA showed these compounds to have optimal binding properties to stack at one end of this quadruplex DNA structure. The aromatic rings of the ligand were shown to be optimally positioned above three of the four guanines of the quartet to favor $\pi-\pi$ stacking interactions. In addition, upon stacking on top of the guanines, the metal center in these complexes is positioned at the center of the quartet (with the potential for helping to neutralize its negative electrostatic charge). As has been reported elsewhere,[39,46] water solubility and strength of interaction between planar delocalized molecules and quadruplex DNA can be increased considerably by attaching substituents such as piperidine to the planar core of the molecule. On the basis of these designs, a series of complexes (with Ni^{2+}, Cu^{2+}, Zn^{2+}, and V^{4+}) was prepared (see Schemes 1−5), and the complexes' interactions with quadruplex and duplex DNA were studied.

Several structural variations were systematically studied. For example, the nature of the substituents on the lower aromatic rings was varied in complexes **3**, **5**, **7**, and **9** (and also in the series **4**, **6**, and **8**). As indicated above, these substituents could not only increase water solubility but also increase binding with the grooves of this quadruplex DNA. We have examined the effects of the size and nature of the cyclic amine and the length of the aliphatic spacer on the binding and solubility properties of the complexes. It was also of interest to establish whether the interaction between the metal complexes and quadruplex DNA would be modified by varying the nature and number of the aromatic rings of the ligands. Complexes **3**, **4**, and **12** should provide some insight into the importance of the central aromatic ring for binding and whether certain substituents could influence the binding properties of the complexes.

Complexes **3**−**9** and **12** were prepared following the synthetic route shown in Schemes 1 and 2. First, complexes **1**, **2**, and **11** were prepared and isolated. This was followed by reaction of the corresponding complex with a range of different alkyl-amino halides (in the presence of K_2CO_3) to yield the final disubstituted compounds (**3**−**9** and **12**). All of the compounds were fully characterized by ^1H NMR and IR spectroscopy, ESI(+) mass spectrometry, and elemental analyses (see the Supporting Information for experimental details). The copper(II) complex **14** was prepared using an analogous synthetic procedure to the one described for the nickel complexes (see Scheme 3).

Since selectivity for the quadruplex versus the duplex is a desirable feature in the design of potential anticancer drugs (which can interact selectively with, for example, telomeric DNA quadruplex structures), it was decided to explore whether metal complexes with square-based pyramidal geometries could also interact via $\pi-\pi$ stacking with the G-quartets of quadruplex DNA. In contrast to the nickel(II) and copper(II) square-planar complexes, square-based pyramidal compounds would only have one available face for interaction with a G-quartet and would not be likely to intercalate between base pairs of duplex DNA. Therefore, they could potentially provide more selective compounds. With this in mind, zinc(II) and vanadyl metal complexes of salphen-type ligands were prepared (see Schemes 4 and 5).It is well-documented that vanadyl complexes with tetra-dentate Schiff bases yield slightly distorted square-based pyramidal species in which the oxo ligand occupies an axial position.[53,54] On the other hand, zinc(II) complexes have a more flexible coordination sphere (due to the closed d^{10} shell of the metal center), and therefore it is not always straightforward to predict the exact geometry of the resulting complexes.

Scheme 3. Synthetic Scheme for the Preparation of Copper(II)−Salphen Complexes

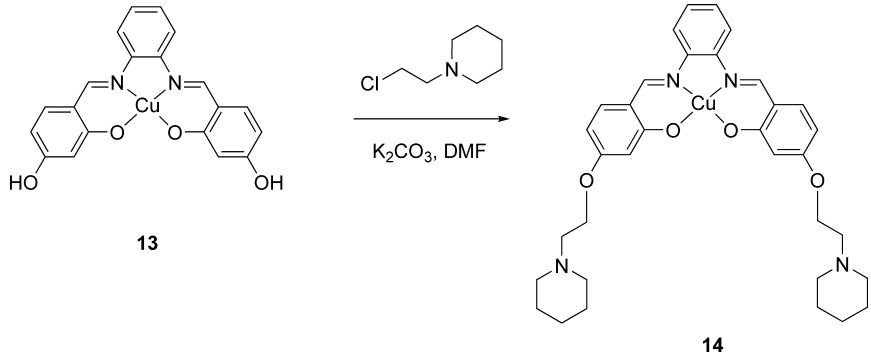

13 **14**

Scheme 4. Synthetic Scheme for the Preparation of Zinc(II)−Salphen Complexes

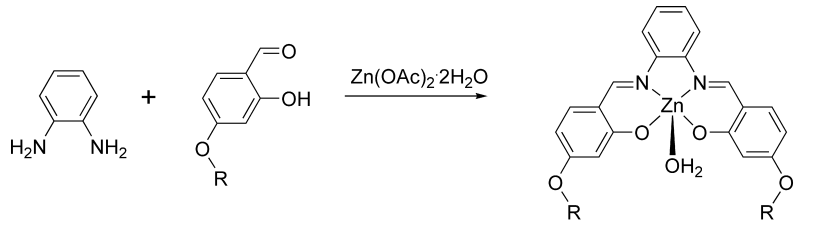

Scheme 5. Synthetic Scheme for the Preparation of Vanadyl−Salphen Complexes

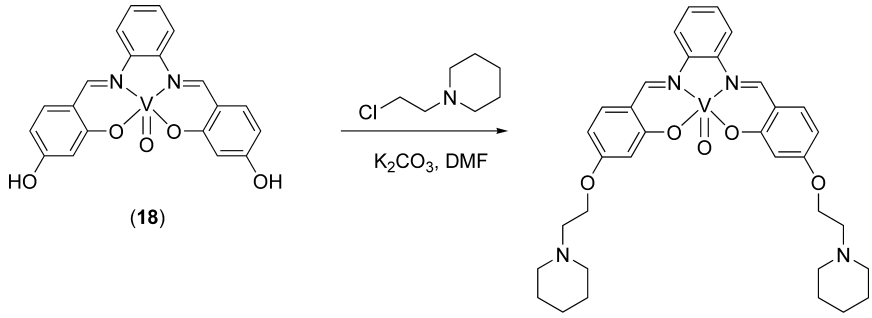

(**18**) (**19**)

Zinc(II) complex **15** was prepared by reacting 2,4-dihydroxobenzaldehyde with 2-aminoaniline in the presence of $Zn(OAc)_2{\cdot}2H_2O$. The ethylpiperidine-substituted complex **17** was prepared by an analogous procedure using 4-substituted 2-hydroxobenzaldehyde. The complexes were characterized by spectroscopic and analytical techniques (see the Supporting Information for experimental details).

Structural Characterization. To confirm the overall structure of the complexes, X-ray crystal structures of **1**, **4**, and **15** were obtained. Complex **1** crystallizes as dihydrate in the space group *C*2/*c* with molecular *C*2 symmetry (see Figure 2). The geometry around the nickel(II) center is square-planar, with the nickel(II) strongly chelated by the tetradentate ligand. The aromatic rings on the molecule are not completely coplanar, with an angle of ca. 9° between the planes defined by the Ni1−O1−C1−C6−C7−N1 ring and the equivalent ring on the opposite side of the molecule. In spite of this slight deviation from planarity, $\pi-\pi$ interactions between neighboring molecules are observed. The centroid···centroid distance between the ring Ni1−O1−C1−C6−C7 from one molecule and the ring C1−C2−C3−C4−C5−C6 from a neighboring one, is 3.57 Å.

Compound **4** crystallizes as a toluene solvate with a disordered fluorine atom. The geometry around the nickel(II) center in **4** is square-planar, with the ligand binding the metal center in a tetradentate fashion (see Figure 3). The aromatic rings on the complex are not completely coplanar, with an angle of ca. 9° between the planes defined by the Ni1−O1−C1−C6−C7−N1 ring and the equivalent ring on the opposite side of the molecule (i.e., Ni1−O2−C20−C15−C14−N2).

(53) Kojima, M.; Taguchi, H.; Tsuchimoto, M.; Nakajima, K. *Coord. Chem. Rev.* **2003**, *237*, 183–196.
(54) Homden, D.; Redshaw, C.; Wright, J. A.; Hughes, D. L.; Elsegood, M. R. J. *Inorg. Chem.* **2008**, *47*, 5799–5814.

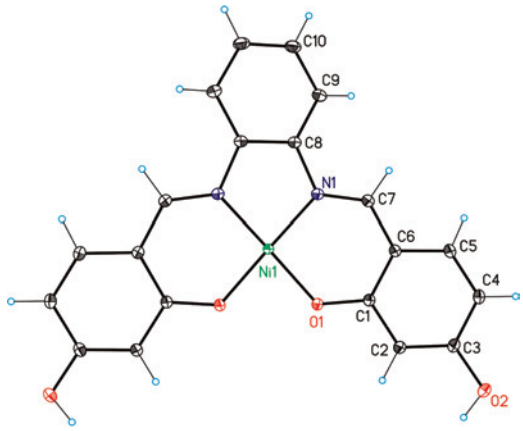

Figure 2. Ortep plot (thermal ellipsoids shown at 50% probability level) of **1** after application of the 2-fold symmetry operation. Water molecules were omitted for clarity.

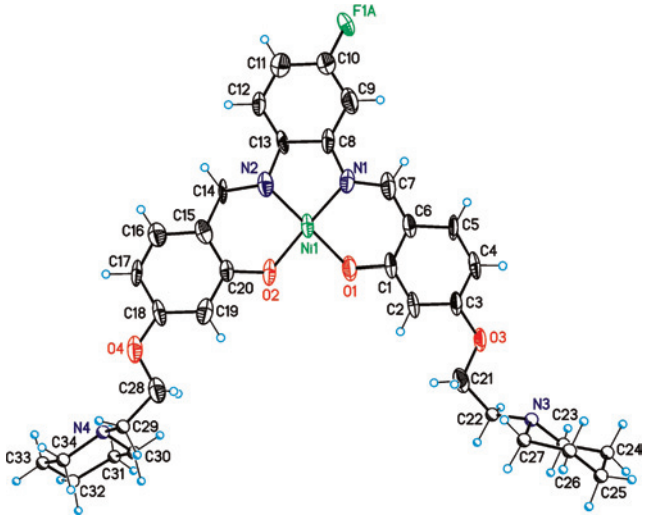

Figure 3. Ortep plot (thermal ellipsoids shown at the 50% probability level) of **4**. The partially disordered piperidine groups are shown in ball-and-stick representation for clarity. Only one of the disordered positions of the fluorine atom is shown.

These two crystallographic studies confirmed that nickel(II) complexes with salphen-type ligands have a nearly planar geometry (based on the square-planar coordination around the metal center). This geometry is in principle favorable for $\pi-\pi$ stacking on top of the G-quartets.

In order to confirm the geometry of the zinc(II) complex, an X-ray crystal structure analysis of **15** was carried out. This revealed that **15** has a distorted square-base pyramidal geometry with a water molecule coordinated in the axial position (see Figure 4). In comparison to the structures of **1** and **4**, in complex **15**, the salphen ligand is much more bent. The planes containing rings Zn1−O1−C1−C6−C7−N1 and Zn1−O4−C20−C15−C14−N2 respectively form an angle of 37°. This "pushes" the zinc center by 0.430(3) Å out of the plane of the base of the pyramid formed by N1−N2−O1−O4, preventing the system from establishing strong $\pi-\pi$ interactions in the solid state.

FRET Studies to Evaluate the Interaction between the Metal Complexes and DNA. The ability of these metal complexes to interact with G-quadruplex DNA F21T (sequence: 5′-FAM-d(GGG[TTAGGG]3)-TAMRA-3′) was first investigated by a FRET melting assay,[55] and the results are summarized in Table 2. These investigations clearly showed that several of the metal complexes under study interact very strongly with this quadruplex DNA. At 1 μM concentrations, the increase in melting temperature (ΔT_m) induced by nickel−salphen complexes **3**−**9** ranges between 26.4 and 31.6 °C. These FRET results for the series **3**−**9** suggest that variations on the cyclic amine substituents (e.g., the alkyl spacer length and amine ring size) do not lead to significant differences in binding within the series. On the other hand, the nickel(II)−salen complex **12** (with an ethyl rather than a phenyl backbone, see Scheme 2) has a lower ΔT_m than the analogous nickel(II)−salphen complexes **3** and **4**. Although this was initially expected since **12** has two rather than three aromatic rings, it is interesting to note that the ΔT_m of 22.9 °C is comparable to that observed for the previously reported tricyclic acridine lead compound BRACO-19. Complex **19**, with a square-based pyramidal geometry, has a ΔT_m of 10.5 °C, which is considerably lower than that of the analogous square-planar complexes. This indicates that, for optimal binding, the complexes must have both their planar "faces" available for $\pi-\pi$ stacking to the guanine quartet. In the case of the zinc complex **17**, with a considerably distorted square-based pyramidal geometry (see Figure 4), binding to quadruplex DNA is negligible at the concentrations studied, highlighting the importance of a planar geometry for optimal stacking between the metal complexes and the guanine quartet.

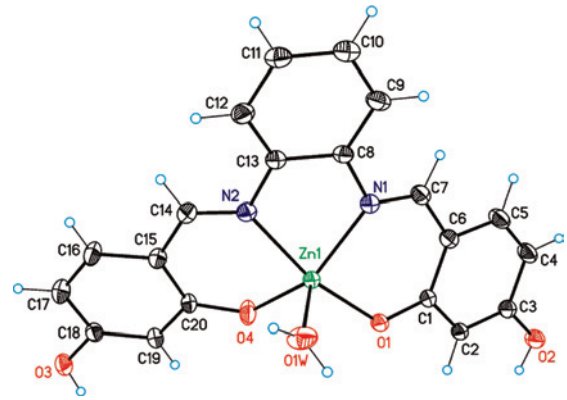

Figure 4. Ortep plot (thermal ellipsoids shown at 50% probability level) of **15**. Noncoordinated water molecules are omitted for clarity.

The interaction of these metal complexes with the duplex DNA sequence 5′-FAM- TATAGCTATA TTTTTT TATAGCTATA-TAMRA-3′ (T_m = 60 °C in the absence of any added compound) was also investigated. As can be seen in Table 2, at the same concentration of the metal complex (1 μM), the ΔT_m for duplex DNA is much lower (in all cases below 2 °C) than that observed for quadruplex DNA.

FRET competition assays[41] were carried out to study further the selectivity displayed by the metal complexes. More specifically, quadruplex DNA ΔT_m's were measured again for a fixed concentration (1 μM) of added complex but this time in the presence of an increasing excess of duplex

(55) Rachwal, P. A.; Fox, K. R. *Methods* **2007**, *43*, 291–301.

Table 2. Stabilization Temperatures (Determined by FRET) of Quadruplex and Duplex DNA in the Presence of Different Metal Complexes

		ΔT_m (°C) at 1 μM			
compound	metal	G4 DNA	dsDNA	[concn] μM, ΔT_m = 20 °C G4 DNA	[concn] μM, ΔT_m = 2 °C dsDNA
3	Ni	31.3	0.1	0.2	4.8
4	Ni	31.5	0	0.1	2.3
5	Ni	31.1	1.7	0.2	1.2
6	Ni	30.5	1.5	0.2	1.4
7	Ni	31.6	0.5	0.1	2.1
8	Ni	28.7	1.7	0.3	1.1
9	Ni	26.4	0	0.3	
12	Ni	22.9	0.4	0.4	3.6
14	Cu	21.5	0	0.7	3.7
17	Zn	1.4	0	4	9.8
19	V	10.5	0.1	4.6	4.2
BRACO-19		21.7	14.5	0.8	0.1

DNA (CT DNA). Measurements for compounds **5** and **7**−**9** were performed with 10 mM potassium cacodylate and 50 mM lithium cacodylate buffers (pH 7.4) in view of the very high quadruplex affinities of these three compounds, while measurements for compounds **12**, **14**, and **19** could be undertaken with a 60 mM potassium cacodylate buffer (pH 7.4). The results of these experiments are summarized in Figure 5; results for the established quadruplex DNA binder BRACO-19 are also presented for comparison.

The results confirm the high selectivity of these metal complexes for quadruplex DNA versus duplex DNA. For complexes **5**, **7**, **8**, and **14**, a slight decrease of the quadruplex DNA melting temperature (*ca*. 4 °C) is observed at a 6 μM concentration of CT DNA (equivalent to a 10-fold excess of CT-DNA). At considerably higher concentrations of CT DNA (120 μM, equivalent to a 200-fold excess of CT-DNA), the quadruplex DNA melting temperature in the presence of this group of complexes is reduced by ca. 10 °C, in comparison to the melting of quadruplex DNA in the absence of CT DNA. Interestingly, with complexes **9**, **12**, and **19** (one of which, **19**, has square-based pyramidal geometry), there is a very small decrease in the melting temperature of quadruplex DNA, even in the presence of a large excess (200-fold) of CT DNA, indicating their high selectivity for quadruplex versus duplex DNA.

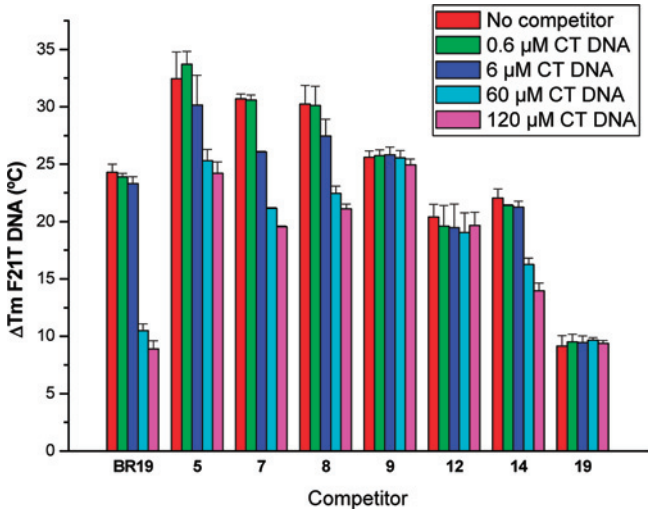

Figure 5. FRET competition experiments of selected complexes at 1 μM concentration showing the reduction of F21T DNA melting temperature with increased concentration of CT DNA.

Table 3. FID ($^{G4}DC_{50}$) Characterization of a Selection of Complexes

compound	$^{G4}DC_{50}$(μM), HteloG4 DNA
7	0.17
12	1.70
14	0.56
17	<10μM
19	1.20

FID Assay. A displacement assay has been employed to measure the interaction of small molecules with quadruplex DNA.[56,57] In this FID assay, TO is mixed with quadruplex DNA, with which it interacts in a single-site manner and with high affinity ($K_a = 3 \times 10^6$ M^{-1}). Upon interaction with quadruplex DNA, this dye displays a significant increase in its fluorescence (up to 3000-fold), whereas when free in solution, the fluorescence is quenched. Therefore, displacement of this dye by another molecule can be used to quantify the affinity of the second molecule toward quadruplex DNA. This is done by calculating the compound concentration at which the fluorescence signal has decreased by 50% (it is assumed that this corresponds to 50% displacement of the TO ($^{G4}DC_{50}$)), allowing for comparisons between different potential quadruplex DNA stabilizers. To confirm the results obtained by FRET, a selection of our complexes was analyzed using FID, and the results are summarized in Table 3.

The results obtained by FID are overall consistent with those obtained by FRET: the square-planar nickel(II) and copper(II) salphen complexes (**7** and **14**) show strong interactions with quadruplex DNA. On the other hand, the square-based pyramidal zinc and vanadium complexes show negligible (**17**) or little (**19**) interaction with quadruplex DNA.

Circular Dichroism. In the presence of potassium cations, human telomeric DNA can exist as a mixture of parallel and antiparallel G-quadruplex conformations. It has been previously shown that certain quadruplex DNA binders can interact preferentially with one of these two conformations.[58−60] In order to study whether the nickel(II)−salphen

(56) Monchaud, D.; Allain, C.; Teulade-Fichou, M. P. *Nucleosides, Nucleotides Nucleic Acids* **2007**, *26*, 1585–1588.
(57) Monchaud, D.; Allain, C.; Bertrand, H.; Smargiasso, N.; Rosu, F.; Gabelica, V.; De Cian, A.; Mergny, J. L.; Teulade-Fichou, M. P. *Biochimie* **2008**, *90*, 1207–1223.
(58) Giraldo, R. ; Suzuki, M. ; Chapman, L. ; Rhodes, D. *Proc. Natl. Acad. Sci. U. S. A.* **1994**, *91*, 7658–62.

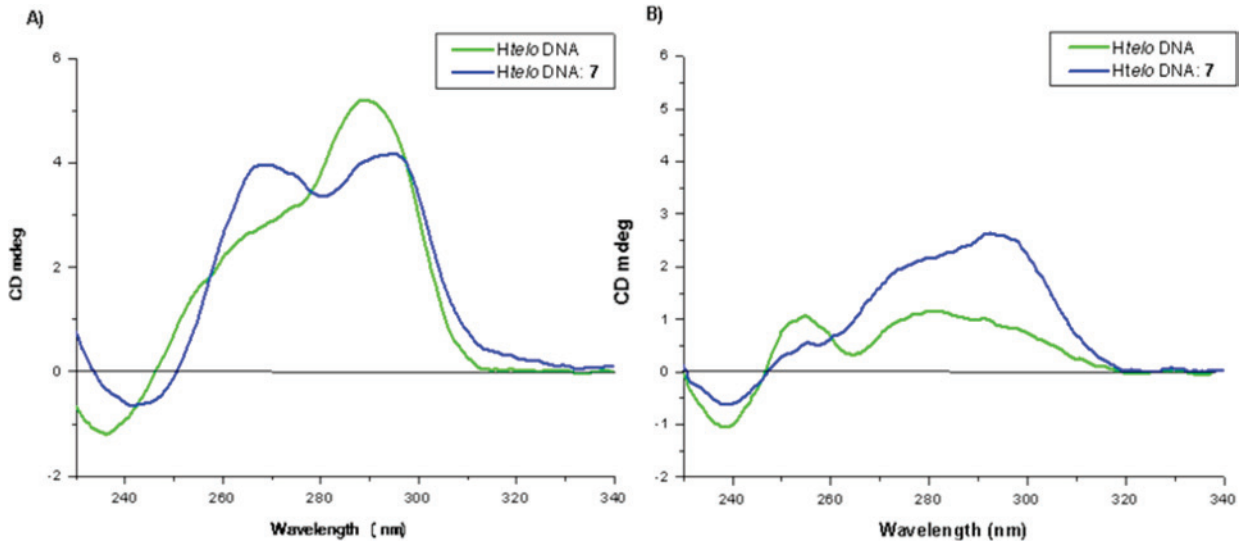

Figure 6. CD spectra of (A) 10 μM Htelo DNA in a 50 mM Tris-HCl and 150 mM KCl, pH 7.4, buffer in the absence and presence of 2 equiv of compound **7**. (B) 10 μM Htelo DNA in a 50 mM Tris-HCl, pH 7.4, buffer in the absence and presence of 2 equiv of compound **7**.

complexes showed this type of selectivity, CD experiments were performed on complex **7**. The experiments were carried out using the Htelo DNA sequence 5′-GG(ATTGGG)$_3$ATTGGG-3′ in 50 mM Tris-HCl and 150 mM KCl buffer (pH 7.4). The CD spectra of Htelo quadruplex DNA (10 μM) showed a significant change in the presence of complex **7** (20 μM), as can be seen in Figure 6A. This complex seems to favor the parallel conformation associated with a positive peak at ca. 265 nm. This is also shown by the decreased intensity of the positive peak with a maximum at around 295 nm (associated with the antiparallel conformation) upon the addition of complex **7**.

We were also interested in establishing whether complex **7** would induce the formation of quadruplex DNA in the absence of potassium cations. This was evaluated by measuring the CD of Htelo DNA in a K^+-free buffer and in the presence of 2 equiv (20 μM) of complex **7**, which showed the decrease of the positive peak at 255 nm (associated with the nonannealed Htelo DNA) and increases of the positive peaks at 265 nm (parallel) and 295 nm (antiparallel) quadruplex DNA. This indicates that complex **7** induces the formation of quadruplex DNA even in the absence of K^+ cations.

Conclusions

A series of metal complexes with Schiff bases has been prepared and fully characterized, including three X-ray crystal structures. These complexes have square-planar or square-based pyramidal structures and the appropriate geometry to $\pi-\pi$ stack onto G-tetrads at the 5′ or 3′ ends of quadruplex DNA structures. The FRET, FID, and CD studies all demonstrate that the planar nickel(II) and copper(II) complexes are highly effective stabilizers of the four-repeat human telomeric DNA intramolecular quadruplex structure; the increases in melting temperature as measured by FRET are among the highest values reported to date for any G-quadruplex ligand. These exceptionally high ΔT_m values are likely to be due in part to the optimal geometric arrangement of the aromatic rings around the central metal ion, which would result in increased $\pi-\pi$ stacking between the G-tetrads and these metal complexes. In addition, coordination of the metal to the poly aromatic ligand results in a reduction of electron density on the rings, which gives a further enhancement of the $\pi-\pi$ stacking interactions.

The ΔT_m value for the copper complex **14**, while high by the standards of most quadruplex ligands, is lower than that for the corresponding nickel complex, even though the former should also have planar coordination around the metal atom. The lower value suggests that there may be an equilibrium with axial hydration of the copper ion, which would tend to reduce quadruplex binding. The inability of the zinc complex **17** to interact effectively with quadruplex DNA can be ascribed to the nonplanarity of the region around the zinc coordination and its penta-coordination, as shown in the crystal structure of **15**. The vanadium complex **19** can also be assumed to be penta-coordinated, although here the pyramidal distortion is expected to be less pronounced than in the zinc(II) compound **17**. Therefore, complex **19** will have a quasi-planar base which is likely to facilitate interaction with the guanine quartet of quadruplex DNA (consistent with the FRET and FID results obtained).

The circular dichroism studies of the interaction between one of the square-planar nickel(II)−salphen complexes and quadruplex DNA suggests that this complex favors the formation of the parallel conformation of human telomeric quadruplex DNA both in the presence and in the absence of K^+, in accord with the crystallographic studies on several ligand−DNA complexes.[10,12,61]

Acknowledgment. The European Union is thanked for a studentship to A.A.-A. The ICIQ Foundation (Spain) is thanked for financial support. We are grateful to Dr. Mekala

(59) Goncalves, D. P. N.; Ladame, S.; Balasubramanian, S.; Sanders, J. K. M. *Org. Biomol. Chem.* **2006**, *4*, 3337–3342.
(60) Zhou, J.; Yuan, G. *Chem.—Eur. J.* **2007**, *13*, 5018–5023.
(61) Parkinson, G. N.; Cuenca, F.; Neidle, S. *J. Mol. Biol.* **2008**, *381*, 1145–1156.

Gunaratnam and Tony Reszka for help with the FRET studies, Dr. Tam T. T. Bui and Prof. Alex F. Drake for collecting the CD spectra, and to CRUK for program grant support at the School of Pharmacy (to S.N.).

Supporting Information Available: Full experimental details for the preparation and spectroscopic/analytical characterization of all compounds. Plots for FRET and FID studies. X-ray crystallographic data and CIF files. This material is available free of charge via the Internet at http://pubs.acs.org. Structures have been deposited with the Cambridge Crystallographic Data Centre (http://www.ccdc.cam.ac.uk; CCDC numbers: 705146−70548)

IC8016547